# Spin-Transfer-Driven Ferromagnetic Resonance of Individual Nanomagnets

J. C. Sankey, P. M. Braganca, A. G. F. Garcia, I. N. Krivorotov, R. A. Buhrman, and D. C. Ralph

*Cornell University, Ithaca, New York 14853, USA*
(Received 4 February 2006; published 5 June 2006)

We demonstrate a technique that enables ferromagnetic resonance measurements of the normal modes for magnetic excitations in individual nanoscale ferromagnets, smaller in volume by more than a factor of 50 compared to individual ferromagnetic samples measured by other resonance techniques. Studies of the resonance frequencies, amplitudes, linewidths, and line shapes as a function of microwave power, dc current, and magnetic field provide detailed new information about the exchange, damping, and spin-transfer torques that govern the dynamics in magnetic nanostructures.

Ferromagnetic resonance (FMR) is the primary technique for learning about the forces that determine the dynamical properties of magnetic materials. However, conventional FMR detection methods lack the sensitivity to measure individual sub-100-nm-scale devices that are of interest for fundamental physics studies and for a broad range of memory and signal-processing applications. For this reason, many new techniques are being investigated for probing magnetic dynamics on small scales, including Brillouin scattering [1] and FMR detected by Kerr microscopy [2], scanning probes [3,4], x rays [5], and electrical techniques [6]. Here we demonstrate a simple new form of FMR that uses innovative methods to both drive and detect magnetic precession, thereby enabling FMR studies for the first time on individual sub-100-nm devices and providing a detailed new understanding of their magnetic modes. We excite precession not by applying an ac magnetic field as is done in other forms of FMR, but by using the spin-transfer torque from a spin-polarized ac current [7,8]. We detect the resulting magnetic motions electrically. We demonstrate detailed studies of FMR in single nanomagnets as small as $30 \times 90 \times 5.5$ nm³, and the method should be scalable to investigate much smaller samples as well. Our technique is similar to methods developed independently by Tulapurkar *et al.* [9] for radio-frequency detection, but we will demonstrate that the peak shapes measured there were likely not simple FMR.

We have achieved the following new results: (i) We measure magnetic normal modes of a single nanomagnet, including both the lowest-frequency fundamental mode and higher-order spatially nonuniform modes. (ii) By comparing the FMR spectrum to signals excited by a dc spin-polarized current, we demonstrate that different dc biases can drive different normal modes. (iii) From the resonance line shapes, we distinguish simple FMR from a regime of phase locking. (iv) From the resonance linewidths, we achieve efficient measurements of magnetic damping in a single nanomagnet.

Our samples have a nanopillar structure [Fig. 1(a), inset], consisting of two magnetic layers—20 nm of permalloy (Py = $Ni_{81}Fe_{19}$) and 5.5 nm of a $Py_{65}Cu_{35}$ alloy—

separated by a 12 nm copper spacer (see details in [10]). We pattern the layers to have approximately elliptical cross sections using ion milling. We focus here on one $30 \times 90$ nm² device, but we also obtained similar results in $40 \times 120$ nm² and $100 \times 200$ nm² samples. We use different materials for the two magnetic layers so that by applying a perpendicular magnetic field $H$ we can induce an offset angle between their equilibrium moment directions (both the spin-transfer torque and the small-angle resistance
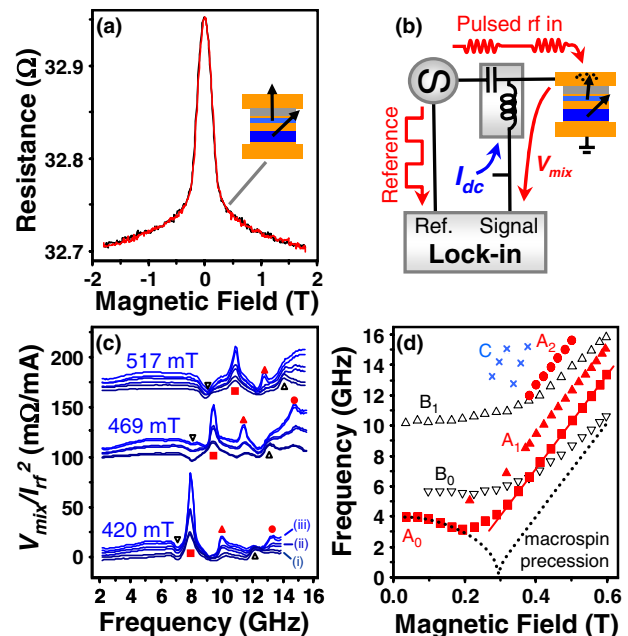


FIG. 1 (color online). (a) Room-temperature magnetoresistance as a function of field perpendicular to the sample plane. Inset: Cross-sectional sample schematic, with arrows denoting a typical equilibrium moment configuration in a perpendicular field. (b) Schematic of circuit used for FMR measurements. (c) FMR spectra measured at several values of magnetic field, at $I_{dc}$ values (i) 0, (ii) 150 $\mu$A, and (iii) 300 $\mu$A, offset vertically. Symbols identify the magnetic modes plotted in (d). Here $I_{rf} = 300$ $\mu$A at 5 GHz and decreases by ~50% as $f$ increases to 15 GHz [10]. (d) Field dependence of the modes in the FMR spectra. The solid line is a linear fit, and the dotted line would be the frequency of completely uniform precession.

response are zero otherwise). The room-temperature mag-
netoresistance [Fig. 1(a)] shows that the PyCu moment
saturates out of plane at $\mu_0 H \approx 0.3$ T, while the larger
moment of Py does not saturate until approximately
$\mu_0 H > 1$ T [11]. All of our FMR measurements are per-
formed at low temperature ($\leq 10$ K), and the direction of $H$
is approximately perpendicular to the layers ($\hat{z}$ direction),
tilted $\sim 5°$ along the long axis of the ellipse ($\hat{x}$ direction) to
control in-plane moment components. Positive currents
correspond to electron flow from the PyCu to the Py layer.
Using a bias tee, we apply current at both microwave
frequencies ($I_{rf} \cos 2\pi f t$) and dc ($I_{dc}$) while measuring
the dc voltage across the sample $V_{dc}$ [Fig. 1(b)]. If the
frequency $f$ is set near a resonance of either magnetic
layer, the layer will precess, producing a time-dependent
resistance:

$$R(t) = R_0 + \Delta R(t) = R_0 + \mathrm{Re}\left(\sum_{n=0}^{\infty} \Delta R_{nf} e^{in2\pi ft}\right), \quad (1)$$

where $\Delta R_{nf}$ can be complex. The voltage $V(t) = I(t)R(t)$
will contain a term involving mixing between $I_{rf}$ and
$\Delta R(t)$, so that the measured dc voltage will be

$$V_{dc} = I_{dc}(R_0 + \Delta R_0) + \frac{1}{2} I_{rf} |\Delta R_f| \cos(\delta_f), \quad (2)$$

where $\delta_f$ is the phase of $\Delta R_f$. The final term enables
measurement of spin-transfer-driven FMR. To reduce
background signals and noise, we chop the microwave
current bias at 1.5 kHz and measure the dc mixing signal
$V_{mix} = V_{dc} - I_{dc}R_0$ using a lock-in amplifier.

In Fig. 1(c) we plot the FMR response $V_{mix}/I_{rf}^2$ measured
for $I_{dc}$ near 0. We observe several resonances, appearing as
either peaks or dips in $V_{mix}$. An applied $I_{dc}$ can decrease the
width of some resonances and make them easier to discern,
as discussed below. By studying the field dependence of
the largest resonances [Fig. 1(d)], we identify two groups
that we will call normal modes $A_0, A_1, A_2$ (solid symbols)
and $B_0, B_1$ (open symbols). Above $\mu_0 H = 0.3$ T, the field
required to saturate the PyCu moment along $\hat{z}$, the frequen-
cies of $A_0, A_1,$ and $A_2$ shift linearly in parallel with slope
$df/dH = g\mu_B\mu_0/h$, where $g = 2.2 \pm 0.1$. As expected
for the modes of a thin-film nanomagnet [13], the mea-
sured frequencies are shifted above that of uniform pre-
cession of a bulk film, $f_{film} = (g\mu_B/h)[\mu_0 H - \mu_0 M_{eff}]$,
with $\mu_0 M_{eff} = 0.3$ T. This $H$ dependence provides initial
evidence that $A_0, A_1,$ and $A_2$ are magnetic modes of the
PyCu layer (additional evidence is presented later). The
other two large resonances, $B_0$ and $B_1$, also shift together,
with a weaker dependence on $H$. This is the behavior
expected for modes of the Py layer, because the values of
$H$ shown in Fig. 1(d) are not large enough to saturate the Py
layer out of plane. To avoid coupling between modes in
different layers, we perform our detailed measurements at
fields where the mode frequencies are well separated. In
addition to these modes, we observe small signals [not

shown in Fig. 1(d)] at twice the frequencies of the main
modes and near frequency sums (modes C).

Based on comparisons to simulations [13,14] and that
the lowest-frequency resonances produce the largest resist-
ance signals, we propose that $A_0$ and $B_0$ correspond to the
lowest-frequency normal mode of the PyCu and Py layer,
respectively. This mode should have the most spatially
uniform precession amplitude (albeit not exactly uniform)
[13,14]. The higher-frequency resonances $A_1, A_2,$ and $B_1$
must correspond to higher-order nonuniform modes. The
observed frequencies and frequency intervals are in the
range predicted for normal modes of similarly shaped
nanoscale samples [13,14].

Next we compare the FMR measurements to spontane-
ous precessional signals that can be excited by $I_{dc}$ alone
($I_{rf} = 0$) [15,16]. The power spectral density of resistance
oscillations for dc-driven excitations at 420 mT is shown in
Fig. 2(a). We examine $I_{dc} > 0$, which gives the sign of
torque to drive excitations in the PyCu layer only [12]. A
single peak appears in the dc-driven spectral density above
a critical current $I_c = 0.3$ mA, and moves to higher fre-
quency with increasing $I_{dc}$. The increase in frequency can
be identified with an increasing precession angle, which
decreases the average demagnetizing field along $\hat{z}$ [12]. At
larger $I_{dc}$, we observe additional peaks at higher $f$ and
switching of the precession frequency between different
values, similar to the results of previous measurements
[12,15,16] that have not been well explained before.

The FMR signals are displayed in Fig. 2(b) at the same
values of $I_{dc}$ shown in Fig. 2(a). We find that the FMR
fundamental mode $A_0$ that we identified above with the
PyCu layer is the mode that is excited at the threshold for
dc-driven excitations. When $I_{dc}$ is large enough that the dc-
driven mode begins to increase in frequency (585 $\mu A$), the
shape of this FMR changes from a simple Lorentzian to a
more complicated structure with a dip at low frequency and
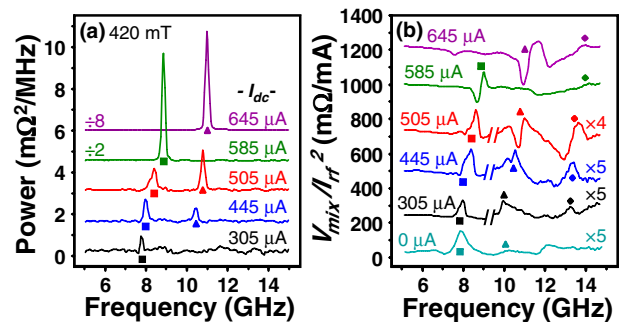a peak at high frequency. The FMR peaks $A_1$ and $A_2$ also

FIG. 2 (color online).  Comparison of FMR spectra to dc-
driven precessional modes. (a) Spectral density of dc-driven
resistance oscillations for different values of $I_{dc}$ (labeled), with
$\mu_0 H = 370$ mT and $I_{rf} = 0$. (b) FMR spectra at the same values
of $I_{dc}$, measured with $I_{rf} = 270$ $\mu A$ at 10 GHz. The high-$f$
portions of the 305 $\mu A$, 445 $\mu A$, and 505 $\mu A$ traces are am-
plified to better show small resonances. The $I_{dc} = 0$ curve is the
same as in Fig. 1(c).

vary strongly in peak shape and frequency as a function of positive $I_{dc}$, in a manner similar to $A_0$, confirming that $A_1$ and $A_2$ (like $A_0$) are associated with the PyCu layer. The FMR modes $B_0$ and $B_1$ that we identified with the Py layer do not shift significantly in $f$ as a function of positive $I_{dc}$. This is expected, because positive $I_{dc}$ is the wrong sign to excite spin-transfer dynamics in the Py layer [7].

There has been significant debate about whether the magnetic modes which contribute to the dc-spin-transfer-driven precessional signals correspond to approximately uniform macrospin precession or to nonuniform spin-wave instabilities [17–20]. Our FMR measurements show directly that, at $I_c$, the dc-driven peak frequency is equal to that of the lowest-frequency rf-driven mode, the one expected to be most spatially uniform [13]. Higher values of $I_{dc}$ can also excite the spatially nonuniform mode $A_1$ and even produce mode hopping so that mode $A_1$ can be excited when mode $A_0$ is not.

In order to analyze the FMR peak shapes, we make the simplifying assumption that the lowest-frequency modes $A_0$ and $B_0$ can be approximated by a macrospin model, with the Slonczewski form of the spin-transfer torque [7]. The small-amplitude resonance is predicted [10] to have a simple Lorentzian line shape,

$$V_{mix}(f) \propto \frac{I_{rf}^2/\Delta_0}{1 + [(f - f_0)/\Delta_0]^2}. \tag{3}$$

Here $f_0$ is the unforced precession frequency. The width $\Delta_0$ predicted for the PyCu layer in our experimental geometry is, to within 1% error for $\mu_0 H > 0.5$ T [10],

$$\Delta_0 = \alpha f_0, \tag{4}$$

where $\alpha$ is the Gilbert damping parameter. As predicted by Eq. (3), we find that the measured FMR peak for mode $A_0$ at $I_{dc} = 0$, for sufficiently small values of $I_{rf}$, is fit accurately by a Lorentzian, the amplitude scales $V_{mix} \propto I_{rf}^2$, and the width is independent of $I_{rf}$, [Figs. 3(a) and 4(a)]. Our minimum measurable precession angle is $\approx 0.2°$. For $I_{rf} > 0.35$ mA, the peak eventually shifts to higher frequency and the shape becomes asymmetric, familiar properties for nonlinear oscillators [21]. From the magnitude of the frequency shift in similar signals [Fig. 3(b), inset], we estimate that the largest precession angle we have achieved is approximately 40°.

The peak shape for mode $B_0$ is also to good accuracy Lorentzian for small $I_{dc}$, but with negative sign. This sign is expected because when the Py moment precesses in resonance, the positive current pushes the Py moment angle closer to the PyCu moment, giving a negative resistance response. The FMR peak shapes for the higher-order modes $A_1$, $A_2$, and $B_1$ are not as well fit by Lorentzians. We plot the spectrum of dc-driven excitations for $I_{dc} = 0.52$ mA, $I_{rf} = 0$ in Fig. 3(b). The width is much narrower than the FMR spectrum for the same mode (inset), confirming arguments that the linewidths in these two types of measurements are determined by different physics [22].
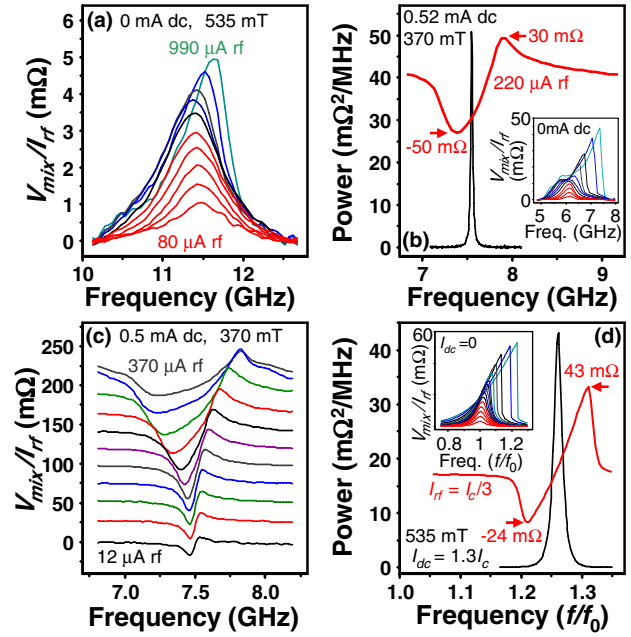


FIG. 3 (color online).   (a) FMR peak shape for mode $A_0$ at $I_{dc} = 0$ and different values of $I_{rf}$: from bottom to top, traces 1–5 span $I_{rf} = 80$–$340$ $\mu$A in equal increments, and traces 5–10 span 340–990 $\mu$A in equal increments. (b) Bottom curve: spectral density of dc-driven resistance oscillations for mode $A_0$, showing a peak with a half width at half maximum $= 13$ MHz. Top curve: FMR signal at the same bias conditions, showing the phase-locking peak shape. Inset: Evolution of the FMR peak for mode $A_0$ at 370 mT, $I_{dc} = 0$, for $I_{rf}$ from 30 $\mu$A to 1160 $\mu$A. (c) Evolution of the FMR signal for mode $A_0$ in the phase-locking regime at $I_{dc} = 0.5$ mA, $\mu_0 H = 370$ mT, for (bottom to top) $I_{rf}$ from 12 to 370 $\mu$A, equally spaced on a logarithmic scale. (d) Results of macrospin simulations for the dc-driven dynamics and the FMR signal [10].

We noted above that the FMR peak shape changes from a Lorentzian to a more complex shape for sufficiently large values of $I_{dc}$. [See the detailed resonance shapes in Figs. 3(b) and 3(c).] This shape change can be explained as a consequence of phase locking between $I_{rf}$ and the large-amplitude precession excited by $I_{dc}$ [23–26]. When the precession frequency increases with precession amplitude, the rf current can force the amplitude on the low-$f$ side of the resonance to be smaller than the equilibrium dc-driven trajectory. Under these conditions, the precession phase locks approximately out of phase with the applied rf current ($\delta_f \approx 180°$), giving negative values of $V_{mix}$. Frequencies on the high-$f$ side of the resonance produce phase locking approximately in phase with the drive and a positive $V_{mix}$. We have confirmed this picture by numerical integration of the macrospin model [Fig. 3(d)] [10]. Recently, Tulapurkar *et al.* [9] measured similar peak shapes, and proposed that they were caused by simple FMR with a torque mechanism different from the Slonczewski theory. We suggest instead that the peak shapes in [9] may be due either to phase locking with thermally excited precession at room temperature (rather
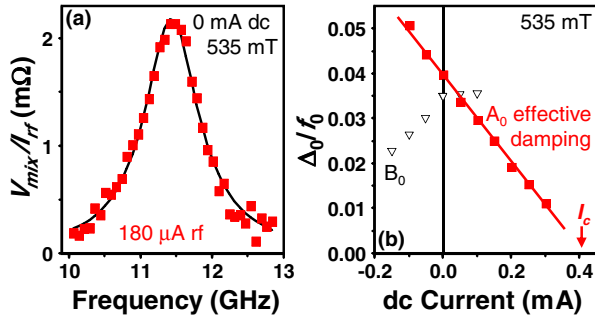
FIG. 4 (color online). (a) Detail of the peak shape for mode $A_0$, at $I_{dc} = 0$, $I_{rf} = 180~\mu$A, $\mu_0 H = 535$ mT, with a fit to a Lorentzian line shape. (b) Dependence of linewidth on $I_{dc}$ for modes $A_0$ and $B_0$, for $\mu_0 H = 535$ mT. For the PyCu layer mode $A_0$, $\Delta_0/f_0$ is equal to the magnetic damping $\alpha$. The critical current is $I_c = 0.40 \pm 0.03$ mA at $\mu_0 H = 535$ mT, as measured independently by the onset of dc-driven resistance oscillations.

than simple FMR), or to the superposition of two FMR signals from different layers (one positive signal like that of $A_0$ and one negative like $B_0$).

A benefit of measuring the Lorentzian line shape of simple FMR is that the linewidth allows a measurement of the magnetic damping $\alpha$, using Eq. (4). It is highly desirable to minimize the damping in spin-transfer-driven memory devices so as to decrease the current needed for switching [7]. Previously, $\alpha$ in magnetic nanostructures could only be estimated by indirect means [27,28]. As shown in Fig. 4(b), for $I_{dc} = 0$ we measure $\alpha = 0.040 \pm 0.001$ for the PyCu layer. This is larger than the damping for $Py_{65}Cu_{35}$ films in identically prepared large-area multilayers as measured by conventional FMR, $\alpha_{film} = 0.021 \pm 0.003$. The cause of the extra damping in our nanopillars is not known, but it may be due to coupling with an antiferromagnetic oxide along the sides of the device [29]. As a function of increasing $I_{dc}$, the theory of spin-transfer torques predicts that the effective damping should decrease linearly, going to zero at the threshold for the excitation of dc-driven precession [7]. This is precisely what we find for mode $A_0$ [Fig. 4(b)]. In contrast, the linewidth of mode $B_0$ decreases with decreasing $I_{dc}$. This is as expected for a Py-layer mode, because the sign of the spin-transfer torque should promote dc-driven precession in the Py layer at negative $I_{dc}$.

We have demonstrated that spin-transfer-driven FMR measurements provide detailed information about the dynamics of both the fundamental and higher-order magnetic normal modes in single sub-100-nm-scale magnetic samples, in both linear and nonlinear regimes. We achieve direct measurements of damping in single nanostructures, show how the damping is tunable by $I_{dc}$, and determine which modes are excited by large dc spin-transfer torques. Spin-transfer-driven FMR will be of immediate utility in understanding and optimizing magnetic dynamics in nano-

structures used for memory and microwave signal-processing applications. Furthermore, both spin-transfer torques and magnetoresistance measurements become increasingly effective on smaller size scales. The same technique may therefore enable new fundamental studies of even smaller magnetic samples, approaching the molecular limit.

[1] S. O. Demokritov and B. Hillebrands, Top. Appl. Phys. **83**, 65 (2002).
[2] S. Tamaru et al., J. Appl. Phys. **91**, 8034 (2002).
[3] M. M. Midzor et al., J. Appl. Phys. **87**, 6493 (2000).
[4] R. Meckenstock et al., Rev. Sci. Instrum. **74**, 789 (2003).
[5] G. Boero et al., Appl. Phys. Lett. **87**, 152503 (2005).
[6] S. E. Russek and S. Kaka, IEEE Trans. Magn. **36**, 2560 (2000).
[7] J. C. Slonczewski, J. Magn. Magn. Mater. **159**, L1 (1996).
[8] L. Berger, Phys. Rev. B **54**, 9353 (1996).
[9] A. A. Tulapurkar et al., Nature (London) **438**, 339 (2005).
[10] See EPAPS Document No. E-PRLTAO-96-047623 for more information about circuit calibration and data analysis. For more information on EPAPS, see http://www.aip.org/pubservs/epaps.html.
[11] The 20 nm Py layer used here has a stronger demagnetizing field than the 3 nm layer of Ref. [12].
[12] S. I. Kiselev et al., Phys. Rev. Lett. **93**, 036601 (2004).
[13] R. D. McMichael and M. D. Stiles, J. Appl. Phys. **97**, 10J901 (2005).
[14] B. Montigny and J. Miltat, J. Appl. Phys. **97**, 10C708 (2005).
[15] S. I. Kiselev et al., Nature (London) **425**, 380 (2003).
[16] W. H. Rippard et al., Phys. Rev. Lett. **92**, 027201 (2004).
[17] M. L. Polianski and P. W. Brouwer, Phys. Rev. Lett. **92**, 026602 (2004).
[18] M. D. Stiles, J. Xiao, and A. Zangwill, Phys. Rev. B **69**, 054408 (2004).
[19] B. Özyilmaz et al., Phys. Rev. B **71**, 140403(R) (2005).
[20] A. Brataas, Y. Tserkovnyak, and G. E. W. Bauer, Phys. Rev. B **73**, 014408 (2006).
[21] L. D. Landau and E. M. Lifshitz, Mechanics (Pergamon, Oxford, 1976), Sec. 29.
[22] J. C. Sankey et al., Phys. Rev. B **72**, 224427 (2005).
[23] W. H. Rippard et al., Phys. Rev. Lett. **95**, 067203 (2005).
[24] S. Kaka et al., Nature (London) **437**, 389 (2005).
[25] F. B. Mancoff et al., Nature (London) **437**, 393 (2005).
[26] M. Tsoi et al., Nature (London) **406**, 46 (2000).
[27] P. M. Braganca et al., Appl. Phys. Lett. **87**, 112507 (2005).
[28] I. N. Krivorotov et al., Science **307**, 228 (2005).
[29] N. C. Emley et al., cond-mat/0510798.